Turkish Journal of Electrical Engineering & Computer Sciences

http://journals.tubitak.gov.tr/elektrik/

Research Article

Turk J Elec Eng & Comp Sci
(2016) 24: 3078 – 3090

doi:10.3906/elk-1405-152

A wavelet-based feature set for recognizing pulse repetition interval modulation patterns

Kenan GENÇOL[1,*], **Nuray AT**[2], **Ali KARA**[1]

[1]Department of Electrical and Electronics Engineering, Atılım University, Ankara, Turkey

[2]Department of Electrical and Electronics Engineering, Anadolu University, Eskişehir, Turkey

Received: 23.05.2014 • **Accepted/Published Online:** 16.02.2015 • **Final Version:** 15.04.2016

Abstract: This paper presents a new feature set for the problem of recognizing pulse repetition interval (PRI) modulation patterns. The recognition is based upon the features extracted from the multiresolution decomposition of different types of PRI modulated sequences. Special emphasis is placed on the recognition of jittered and stagger type PRI sequences due to the fact that these types of PRI sequences appear predominantly in modern electronic warfare environments for some specific mission requirements and recognition of them is heavily based on histogram features. We test our method with a broad range of PRI modulation parameters. Simulation results show that the proposed feature set is highly robust and separates jittered, stagger, and other modulation patterns very well. Especially for the stagger type of PRI sequences, wavelet-based features outperform conventional histogram-based features. Advantages of the proposed feature set along with its robustness criteria are analyzed in detail.

Key words: Electronic warfare, radar intercept systems, pulse repetition interval modulation, feature extraction, wavelet transforms, support vector machines

1. Introduction

In dense signal environments where a large number of (many) emitters can be active simultaneously, a radar intercept system receives an interleaved stream of pulses in the natural time of arrival order. It is then the task of the intercept system to deinterleave this mixed pulse sequence and thus to identify the source emissions. For this identification task, various parameters such as pulse frequency (PF), pulse width (PW), pulse amplitude (PA), angle of arrival (AOA), and time of arrival (TOA) are measured and emission sources are classified accordingly. Among these pulse parameters, TOA is of considerable interest since it leads to a key derived parameter called pulse repetition interval (PRI), which represents the difference of sequential TOAs of received pulses. Any emission source either intentionally or unintentionally varies (or modulates) this parameter for a specific mission requirement. Thus, it is important to recognize PRI modulations for identification of the emission source and its mission for possible countermeasures. Additionally, some emitters may vary even PRI modulation type according to its mission. This makes estimation of PRI modulations more critical from an operational point of view. As the subject is sensitive and may require mostly classified data, it is not possible to see so many works toward resolving this problem.

In the literature, deinterleaving pulse trains have been in the focus of many studies in the past years [1–10]. Several studies were performed on estimation of PRI to construct better deinterleaving algorithms.

*Correspondence: gencol.kenan@gmail.com

Cumulative differences (C-DIF) and sequential differences (S-DIF) histogram techniques, techniques based on TOA matrix characteristics, and a transformation called PRI transform, leading to a kind of PRI spectrum, were some of these algorithms that enabled new methodologies to estimate pulse repetition intervals of pulse sequences and thus to deinterleave them [7–10]. However, as signal environments become more complex in electronic warfare due to the evolution of technology, the need for not only estimating pulse repetition intervals of radar pulses but also recognizing the modulation patterns hidden inside them has become an inevitable task. In recent years, studies have been focused on this area and several methods have been proposed to recognize PRI modulation types [11–18]. In the work of Noone [11], an N-dimensional feature vector was deduced by using the second differences of the TOAs of a pulse train and PRI modulation types are classified via a neural network. In the work of Rong et al. [12], a two-dimensional feature vector was formed by extracting frequency and shape features from this N dimensional vector, which reduced the computation time greatly. In the work of Ryoo et al. [13], PRI modulation types were recognized based on the features extracted from the autocorrelation of the PRI sequences for each PRI modulation type. In this method, due to the sensitivity of the features against signal imperfections, compensation of missing pulses and the removal of spurious pulses must be performed as a preprocessing step. In the work of Kauppi et al. [14], PRI modulation patterns were classified hierarchically. First, six modulation patterns were first grouped into three subpatterns by using a neural network classifier, and then they were binary classified by using one-dimensional classifiers. Some proposed features in this method were based on sequential difference (SDIF) histograms [8] and they need to be calculated for several orders due to unknown signal parameters.

In this study, we present new features based on the wavelet analysis of PRI modulation patterns to classify PRI modulation types. Features are extracted from multiresolution decomposition [19] of the second difference of the TOA signals by utilizing a discrete Haar wavelet. Experimental results show that the extracted features separate jitter, stagger, and other modulation types very well and they are highly robust to real-world imperfections such as missing pulses, spurious pulses, and TOA noise.

The rest of the paper is organized as follows: in Section 2, the basic PRI modulation types and their parameters are given. In Section 3, the proposed feature set and the method are described. Section 4 shows simulation results and discusses these results. Finally, Section 5 concludes this paper.

2. PRI modulation

Let F be a function describing the PRI modulation type:

$$x_n = y_{n+1} - y_n = F(n) \quad n = 1, 2, ..., N-1, \tag{1}$$

where y_n is the TOA of the nth pulse received in a pulse sequence of length N and x_n is the difference of TOAs of two consecutive pulses.

In general, there are six common PRI modulation types: stable, jittered, stagger, dwell & switch, sliding, and periodic. Each modulation type serves for a specific purpose; thus, they represent some characteristics of emitters. Constant PRI means the peak variations in PRI values are less than about 1% of the mean PRI, whereas jittered PRI has large intentional PRI variations up to about 30% of the mean PRI. Staggered PRI uses two or more PRIs selected in a fixed sequence. The sequence may contain more than one of the several intervals before it repeats. In dwell & switch PRI, the radar has bursts of pulses with several stable PRIs switched from one burst to the next. Sliding PRI is characterized by monotonically increasing or decreasing PRI followed by a rapid jump from one extreme value to the other. Finally, periodic PRI means that modulation is a nearly

sinusoidal variation over a more limited range than in sliding PRI. Common PRI modulation types and their parameterizations are presented in Table 1.

Table 1. Common PRI modulation types and their parameterizations.

Constant	$F(n) = c, n = 2, ..., N-1$	c : a constant real number.
Stagger	$F(i+kM) = F(i) \quad i = 1, 2, ..., M$ $k = 1, 2, ..., T$	M: the number of positions in one period T: the number of periods in the pulse sequence Total number of pulses in the pulse sequence is $N = MT$
Dwell and switch	First stage: $F(i) = F(1) \quad i = 2, ..., N_0$ Other stages: $F(i) = F(1 + N_j)$ $j = 0, 1, ..., M-1$ $i = N_j + 2, ..., N_{j+1}$	M : the number of stages in the pulse sequence N_i: the number of pulses in the ith stage The total number of pulses in the pulse sequence is $N = \sum_{k=0}^{M-1} N_k$
Jittered	$F(n) = T + \varepsilon_{Gauss}$	T: the mean PRI ε_{Gauss}: a random variable that has a Gaussian distribution with zero mean and σstandard deviation
Sliding	$F(n) = \alpha(n - 1 \bmod M) + \beta$	M: the number of pulses in one slide period β : the minimum PRI (Min_ pri) value α = (Max_ pri – Min_ pri) / (M-1), the slope of the modulation
Periodic	$F(n) = T + A\sin(wn + \phi)$	T : the mean PRI A :the modulation amplitude (generally up to 5% of mean PRI), w :the modulation frequency (generally between 20 and 50 pulses per period) φ : the phase

3. Methodology

It has been shown that the multiresolution signal decomposition scheme proposed in [19] can be applied to PRI estimation in intercept receivers. In doing this, variations of wavelet coefficients are closely related to PRI modulation patterns obtained from the time sequences of interleaved pulses. Classical multiresolution concept-based multichannel filter banks are adopted to PRI estimation in this work.

After detailed analysis of PRI modulation types via their wavelet decompositions, it was observed that local extrema of the wavelet coefficients of jittered type modulation patterns tend to have lower magnitudes compared to stagger type modulation patterns. This is due to the fact that in staggered sequences, PRI variation is done from pulse to pulse. The radar emitter staggers from one position to another abruptly. These abrupt changes are more likely to be reflected in magnitude to their detail coefficients in contrast to jittered sequences where PRI variation is within a predefined limited range. The medians of the wavelet coefficients of other PRI modulation patterns (stable, dwell & switch, sliding, and periodic) also tend to have lower values compared to jittered and stagger type modulation patterns. Smooth variations of those type patterns cause most of their detail coefficients to tend to zero or to very low numbers in magnitude as compared to jittered and stagger type patterns. These observations gave us a chance to extract new features to distinguish among jittered, stagger, and other PRI modulation types.

Radar intercept systems may encounter a continuous stream of pulses accompanied by many imperfections, and they are required to work on a real-time basis. Since the Haar wavelet is computationally efficient and can be implemented in a transformation matrix form, it has been preferred in our study.

Feature analysis is performed on the second difference of TOAs by utilizing discrete

Haar wavelets.

The Haar wavelet is defined as [20]:

$$\Psi(t) = \left\{ \begin{array}{ll} 1, & 0 \le t < \frac{1}{2} \\ -1, & \frac{1}{2} \le t < 1 \\ 0, & \text{elsewhere} \end{array} \right\}, \tag{2}$$

and the whole set of basis functions is obtained by dilation and translation:

$$\Psi_{m,n}(t) = 2^{-m/2}\Psi(2^{-m}t - n), m, n \in \mathrm{Z}. \tag{3}$$

We call m the scale factor, since $\psi_{m,n}(t)$ is of length 2^m, while n is called the shift factor, and the shift is scale-dependent ($\psi_{m,n}(t)$ is shifted by $2mn$). The normalization factor $2^{-m/2}$ makes $\psi_{m,n}(t)$ of unit norm.

The discrete case of the wavelet can be expressed as:

$$g_{j,k}(n) = 2^{-j/2}g(2^{-j}n - k) \quad k, n \in Z, j \in N. \tag{4}$$

Here, the wavelet filter $g(n)$ plays the role of $\psi(t)$.

The second difference of TOAs is defined by differentiating the modulation function F according to Noone [11]:

$$z_n = x_{n+1} - x_n \quad n = 1, 2, ..., N - 2, \tag{5}$$

where z_n is the second difference of the time of arrival of the nth pulse. Then the detail coefficients of the wavelet decomposition of z_n at scale 2^j can be expressed as:

$$c_d(j, k) = \sum_n z_n g_{j,k}(n). \tag{6}$$

3.1. Analysis of jittered and stagger PRI modulation types

Two features are extracted from the wavelet decomposition of the vector of second differences z_n, of length M as follows:

Let E_i be the square summable energy in the ith level or the ith subband of wavelet decomposition of z_n (d^2TOA), i.e.

$$E_i = \sum_j \left\| c^i \{j\} \right\| = \sum_j \left(c^i \{j\} \right)^2 j = 1, 2, ..., M/2^i, \tag{7}$$

where $c^i\{j\}$ denotes the jth detail coefficient of the ith level decomposition.

The first feature is defined as a vector of the energies in L levels:

$$f_1 = [E_1 \quad E_2 ... E_L], \tag{8}$$

where L is the effective number of decomposition levels, which is analyzed in the next section.

The second feature is the magnitude of the median of wavelet coefficients in the first subband:

$$f_2 = abs(median\{c\{j\}\}) \quad j = 1, 2, ..., M/2. \tag{9}$$

M is assumed to be a multiple of 2, which allows fast wavelet decomposition of the signal.

For classification tasks, we employ a cascaded form of a one-dimensional binary classifier and a support vector machine (SVM) classifier. SVMs are from a class of supervised learning algorithms that can be applied to classification or regression.

The SVM algorithm is based on the statistical learning theory developed by Vapnik [21]. It was originally designed to solve two-class problems (binary classification), but it can be easily extended to solve multiclass problems with combinations of binary classifiers. The goal of the algorithm is to determine the optimum hyperplane that separates two classes. More treatment of SVM theory is beyond the scope of this paper and can be found in [22]. For now, it should be pointed out that major advantages of SVM are that different learning machines can be constructed by utilizing different kernels and nonlinear classification problems can be solved by linear classifiers via mapping to higher dimensional spaces without explicitly modifying the kernels [23].

We first separate the jittered and stagger modulated patterns from others by using a binary classifier. Then a SVM classifier is used to separate the jittered and stagger types. We use a linear kernel for evaluating the performance of our SVM classifier.

3.2. Analysis of other PRI modulation types

The sample kurtosis of wavelet coefficients in the ith subband is given by:

$$Kurt(c^i) = \frac{\frac{1}{M/2^i}\sum_{j=1}^{M/2^i}(c^i\{j\} - \mu_c^i)^4}{(\frac{1}{M/2^i}\sum_{j=1}^{M/2^i}(c^i\{j\} - \mu_c^i)^2)^2}, \tag{10}$$

where c^i is the wavelet coefficients and μ_c^i is the sample mean of the wavelet coefficients in the ith subband, respectively.

Also, let the number of local extrema of wavelet coefficients in the first subband be symbolized as *local extrema* (c^1). Then the hybrid feature:

$$f_3 = \left[Kurt(c^1) \quad Kurt(c^2) \quad Kurt(c^3) \;\; \text{localextrema}(c^1)\right], \tag{11}$$

is very efficient in separating dwell & switch, sliding, and sinusoidal PRI modulation types. For the sake of illustration of the separating capability of the proposed feature, three kurtosis components of this feature are depicted in the next section.

A generalized block diagram of the proposed method is presented in Figure 1.

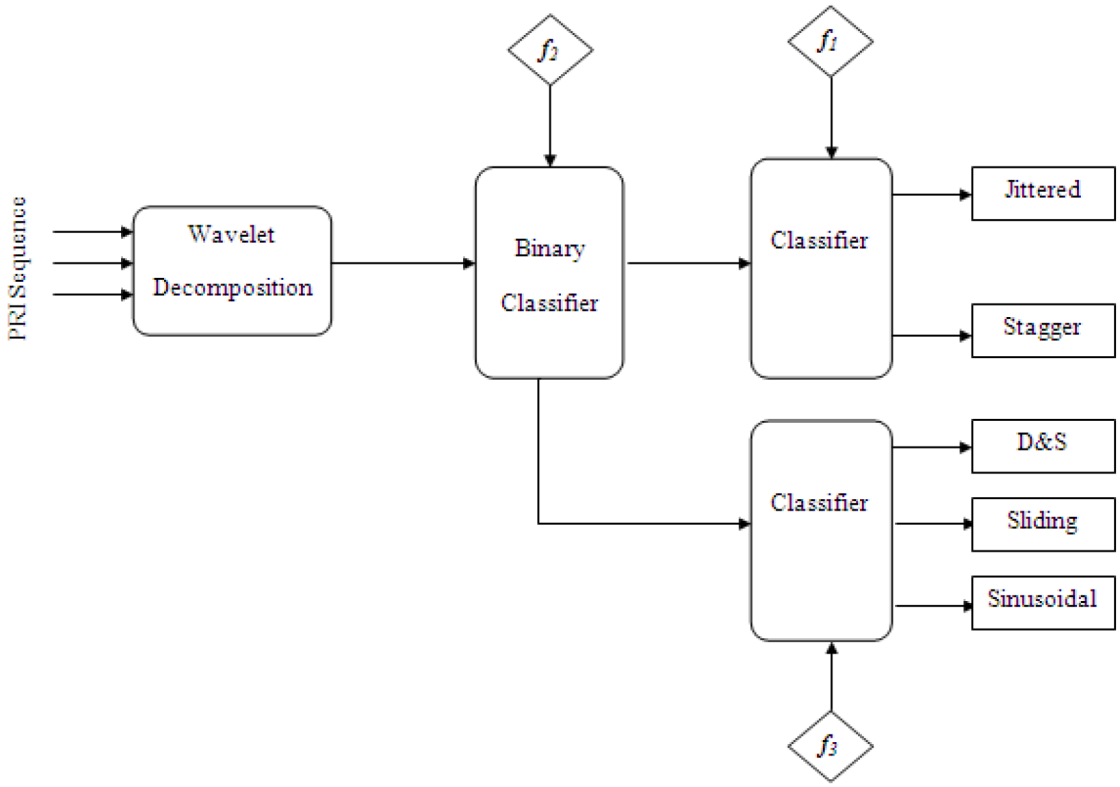

Figure 1. A generalized block diagram of the proposed method.

4. Simulations

The data generation model proposed by Kauppi et al. [14] has a very high flexibility in modulation parameters and is quite adequate for the generation of different PRI modulation sequences. The parameter limits used for data generation are given in Table 2. We train our SVM classifier for a scenario of average missing and spurious pulses of 5%, TOA noise of 0.3%, and a very broad range of training data, where limits are presented in Table 2.

Table 2. The parameter limits for synthetic data generation.

PRI modulation types	Parameters	Range
Jittered	Jitter type Standard deviation	Gaussian, uniform 5%–50%
Stagger	Number of positions	2–64
Dwell & switch	Number of bursts Length of one burst	2–64 8–100
Sliding	Max-min ratio Number of periods	2–20 1–20
Periodic	Amplitude deviation Number of periods	4%–50% 8–100
Imperfections Missing pulses Spurious pulses TOA uncertainty		 0%–15% 0%–15% 0%–0.4%

We have created the test sequence from a broad range of PRI modulation parameters to test the separating capability of the feature set. The test sequence consists of six different types of PRI sequences and their subsequences. Table 3 shows parameters of each PRI sequence. For each PRI sequence, subsequences are formed in such a way that they fully cover the limits of modulation parameters to ensure as unbiased of a sample space as possible and to see the robustness of the features against large variations of modulation parameters of PRI types.

Table 3. Test sequence.

PRI sequence	Subsequences
Constant	10 subsequences
Jittered	46 subsequences of standard deviations 5% to 50% and each subsequence has Gaussian and uniform distributions
Stagger	63 subsequences of stagger positions 2 to 64
Sliding	19 subsequences of max:min ratios 2 to 20 and each subsequence with periods 1, 5, 10, 20
Dwell-switch	15 subsequences of number of bursts 2 to 16 and each subsequence with burst lengths 8, 20, 50, 100
Periodic	47 subsequences of amplitude deviations 4% to 50% and each subsequence with periods 8, 20, 50, 100

For the sake of illustration of separating capability of the feature set, we simulated our training data where parameter limits are presented in Table 2. The separating capabilities of the proposed features are illustrated in Figure 2, Figure 3, and Figure 4, respectively.

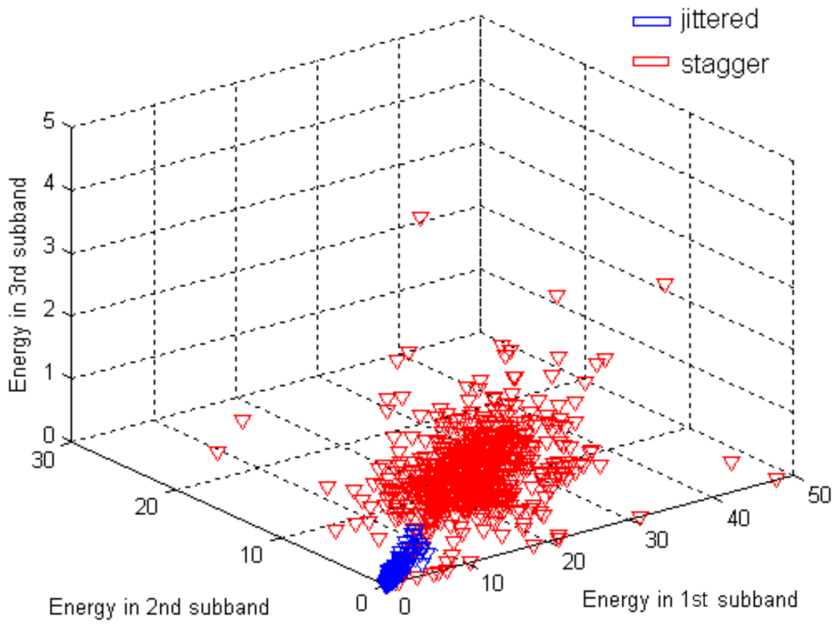

Figure 2. Demonstrating separating capability of the energy feature.

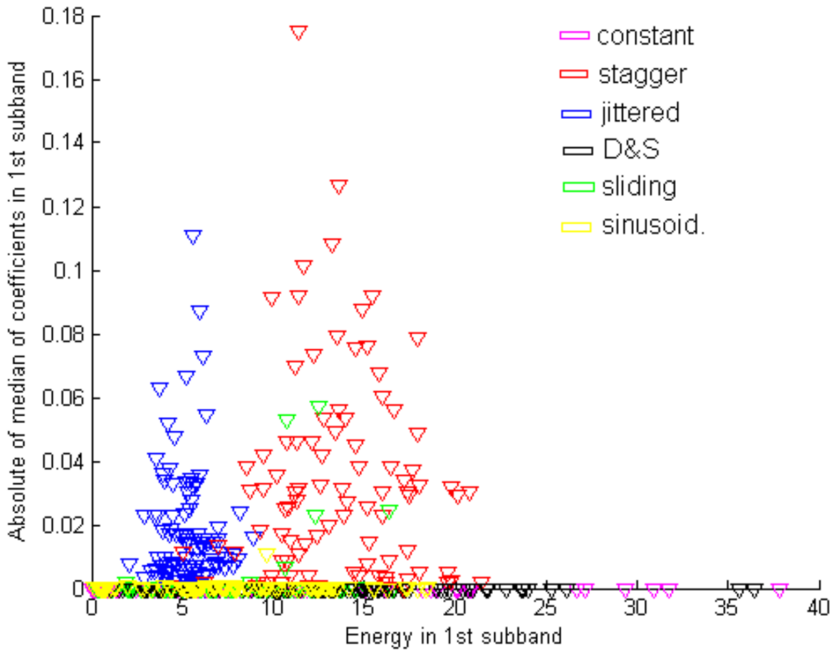

Figure 3. Demonstrating separating capability of the median feature.

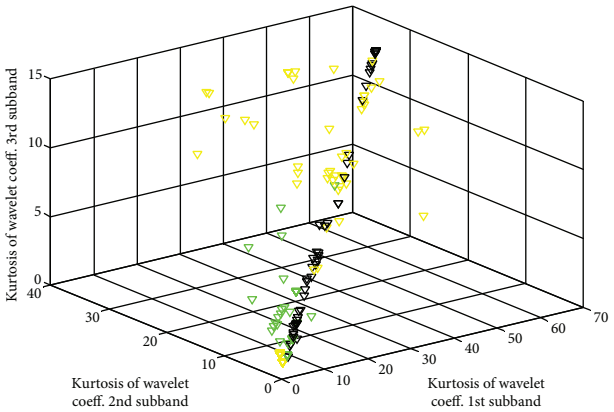

Figure 4. Demonstrating separating capability of three kurtosis components of the 3rd feature.

Tests are performed for four distinct circumstances: in the case of no imperfections, missing pulses case, spurious pulses case, and in the case of TOA noise. For missing and spurious pulses cases, tests are performed ten times and in the case of TOA noise, the trials are increased to 100 to reflect the statistics of noise as much as possible by varying the pulse repetition interval of PRI modulation types and the average recognition rate is calculated. Computation results are obtained on a standard Pentium Dual Core 2 GHz PC with MATLAB R2013a version.

The selection of L (the number of decomposition levels in the first feature) is crucial for the separating capability of the feature for jittered and stagger modulated types. A comparison of the results of Haar and Daubechies wavelets [24] for a typical scenario of average missing and spurious pulses of 5% and TOA noise of 0.3% is given in Table 4. It is observed that average recognition rates of jittered and stagger sequences are very similar for both wavelets and the performance is greatly improved at two and three levels.

Table 4. A comparison of the results of Haar and Daubechies wavelets (M = 128).

PRI modulation patterns	Average recognition rate of PRI modulation patterns					
	Haar wavelet			Daubechies wavelet 'db2'		
	L = 1	L = 2	L = 3	L = 1	L = 2	L = 3
Jittered	72	83	85	70	82	84
Stagger	99	98	98	97	98	99
Computation time (ms)	1.904	2.563	2.959	2.075	2.686	3.206

The average recognition rates of PRI modulation patterns are given in Table 5. It can be inferred from the results that jittered and stagger PRI modulation types have high recognition rates, usually around 95%, except that the recognition performance of jittered type sequences decreases rapidly as the percentage of missing pulses increases. They are not robust to missing pulses. This can be considered the only major shortcoming of the proposed method. Also, other modulation types have average recognition rates of 85%, except in the presence of TOA noise of 0.3% and 0.4%, when they are then 81% and 70%, respectively. Even if they decrease gradually, they still show good performance at tolerable TOA noise rates. One of the major advantages of the proposed features is that they are able to separate stagger type modulation sequences with an accuracy of around 99%. Features show great robustness to real-world imperfections such as missing pulses, spurious pulses, and TOA noise. This property is further analyzed in the next subsections.

Table 5. Classification results (L = 3).

PRI modulation patterns	Average recognition rates of PRI modulation patterns (%)									
	No imperfections	Missing pulses (%)			Spurious pulses (%)			TOA noise (%)		
	imperfections	5	10	15	5	10	15	0.2	0.3	0.4
Jittered	99.35	86.85	72.39	60.43	96.30	91.96	85.20	99.11	99.08	99.00
Stagger	99.21	99.52	99.37	99.21	99.53	99.50	99.36	98.95	98.90	98.22
Others	100	93	86	82	95	91	80	92	80	70

4.1. Comparison with histogram-based methods

In [14], jittered and stagger type PRI sequences are recognized by using histogram-based features. The feature is extracted from higher order SDIF histograms and is defined as the relative strength of a stable sum in the d*th* order SDIF-histogram.

The average recognition rates of jittered and stagger PRI modulation type sequences against missing and spurious pulses are given in Figure 5 and Figure 6, respectively. It is observed from Figure 4 that for jittered type sequences, histogram-based features perform better than wavelet-based features. The average recognition rate of jittered sequences based on histograms is above 80%, while this rate decreases to 60% for the extreme case of 15% missing pulses when wavelet features are employed. For stagger type sequences, wavelet-based features outperform histogram-based features.

In the spurious pulses case (Figure 6), for both jittered and stagger type sequences wavelet-based features perform better than histogram-based features. For jittered sequences, the average recognition rates of both methods are above 85%, while for stagger sequences the average recognition rates based on histograms decrease very quickly. This is due to the dynamic range of the histogram-based feature proposed in [14] for stagger type sequences rapidly increasing when the number of missing or spurious pulses increases.

Histogram-based features also have some bottlenecks. First, since the number of positions of a stagger type sequence is generally unknown due to the unknown signal parameters, the feature needs be calculated up

to several orders [14]. Second, the relative tolerance defining the constant time interval in the histogram stabilization algorithm is a choice parameter that should be updated for dynamically varying signal environments.

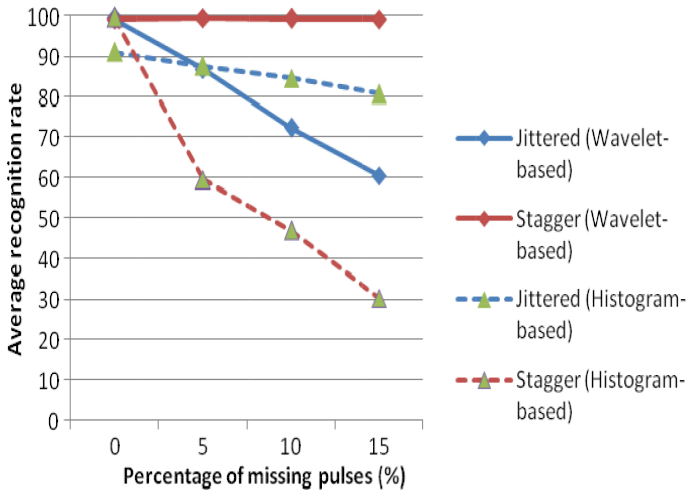

Figure 5. Average recognition rate of histogram and wavelet-based features against missing pulses.

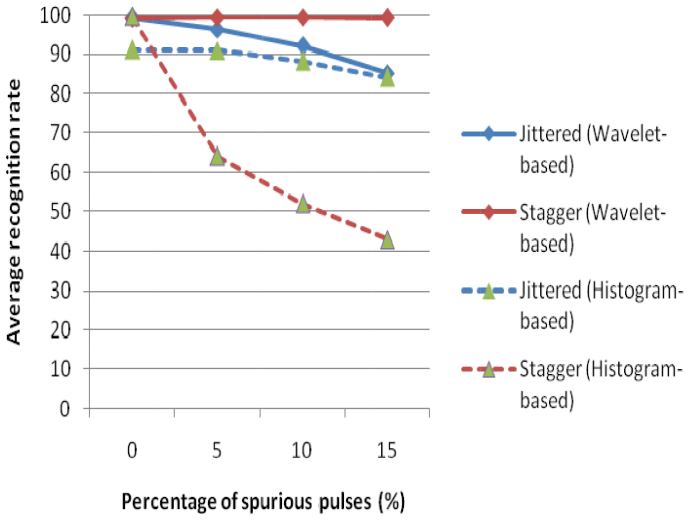

Figure 6. Average recognition rate of histogram and wavelet-based features against spurious pulses.

A comparison of the runtimes of the proposed and histogram method is presented in Table 6. With this comparison, a superior side of the proposed method has been observed. Since the number of positions in stagger PRI is generally unknown, histogram-based features are calculated according to the highest expected number of positions in stagger PRI [14]. A general staggered PRI sequence can contain up to 64 positions as presented in Table 2. On the other hand, wavelet-based features do not depend on the number of positions in stagger PRI, yielding much better run-time performances as seen from Table 6.

Table 6. A comparison of the runtime performance of proposed and histogram methods.

Runtime performance for proposed and histogram methods (ms) (M = 128)						
Number of stagger positions	2	4	8	16	32	64
Histogram	8.686	9.250	9.544	10.535	11.764	12.970
Proposed	2.886 (does not depend on stagger positions)					

4.2. Robustness criteria

One of the most important contributions of this work is that the wavelet features proposed are very robust for stagger type sequences and distinguish them very well as shown in Table 5. Figure 7, Figure 8, and Figure 9 show the dynamic range of the energy feature for stagger sequences with number of positions 2 to 64 against increasing number of missing pulses, spurious pulses, and TOA noise percentages, respectively. It is observed that the dynamic range of the energy feature against signal imperfections does not change significantly and the calculated energy feature values vary between 10 and 25. It should be emphasized that energy feature values calculated for jittered sequences are low and this explains the high recognition performance of stagger type sequences in the circumstances of missing and spurious pulses.

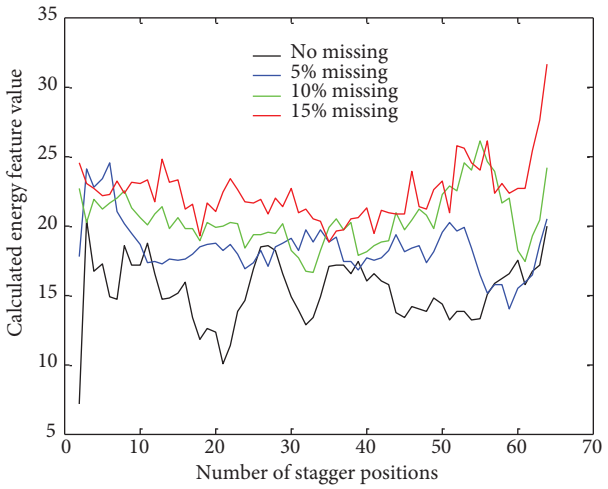

Figure 7. Robustness of energy feature against increasing missing pulses.

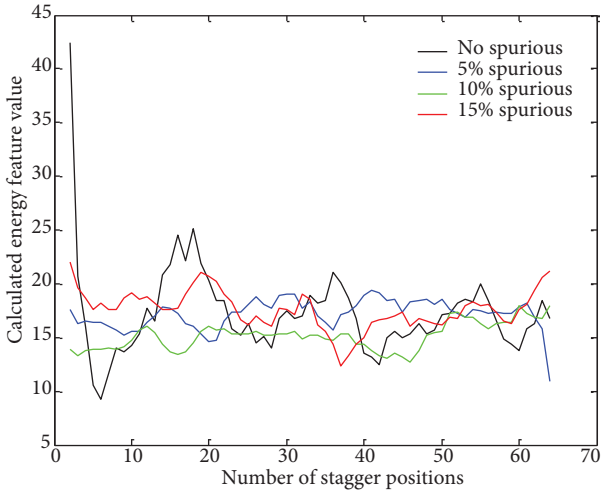

Figure 8. Robustness of energy feature against increasing spurious pulses.

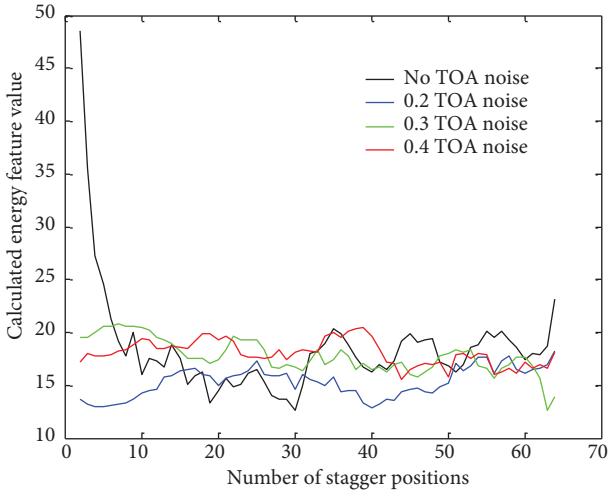

Figure 9. Robustness of energy feature against increasing TOA noise.

It is observed from Table 5 that both jittered and stagger type PRI sequences are highly robust to TOA noise and have average recognition rates of about 98% even in the extreme case of 0.4% noise. This is due to

the fact that the wavelet features are invariant to noise. This property is depicted in Figure 10 and Figure 11 for jittered and stagger sequences, respectively. For the jittered sequence, jittered sequence with jitter deviation of 20% is modeled. For the stagger sequence, a stagger sequence of 4 positions is modeled.

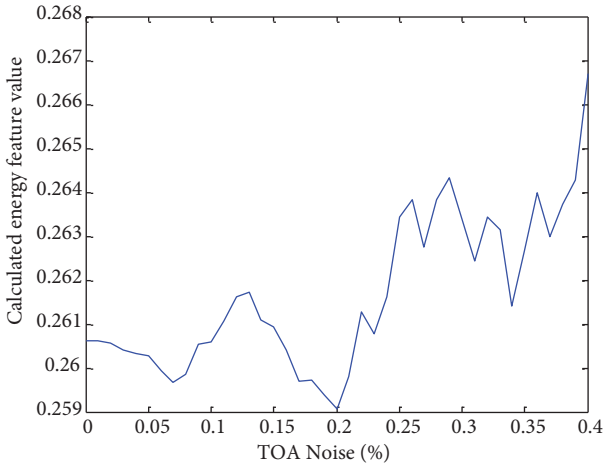

Figure 10. Variation of the energy feature calculated against increasing TOA noise for a jittered type PRI sequence.

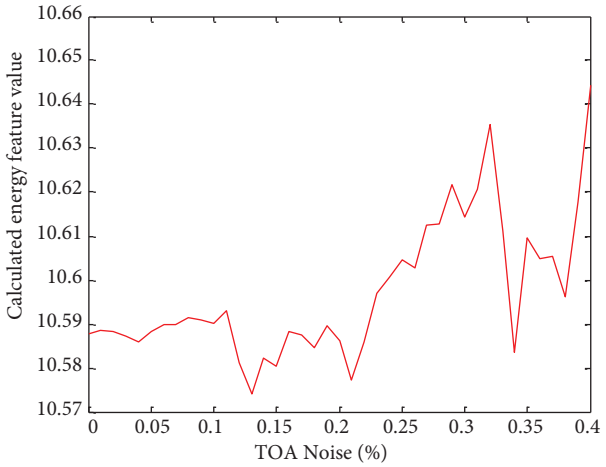

Figure 11. Variation of the energy feature calculated against increasing TOA noise for a stagger type PRI sequence.

It can be inferred from Figures 10 and 11 that for both jittered and stagger sequences the dynamic range of the feature is nearly constant against increasing TOA uncertainty.

5. Conclusion

In this study, we developed a wavelet-based feature set to recognize PRI modulation patterns. Three wavelet features that span the full domain of common PRI modulation types were found to be distinctive to discriminate between jittered, stagger, and other PRI modulation type sequences. The proposed features and the classification method are very effective, especially for emitters that vary PRI patterns continuously. Simulation results show that the separating capability of the proposed features is pretty good and the method is encouraging for the problem of recognizing different PRI modulation patterns.

References

[1] Moore JB, Krishnamurthy V. Deinterleaving pulse trains using discrete-time stochastic dynamic-linear models. IEEE T Signal Proces 1994; 42: 3092-3103.

[2] Logothetis A, Krishnamurthy V. An interval-amplitude algorithm for deinterleaving stochastic pulse train sources. IEEE T Signal Proces 1998; 46: 1344-1350.

[3] Conroy TL, Moore JB. The limits of extended Kalman filtering for pulse train deinterleaving. IEEE T Signal Proces 1998; 46: 3326-3332.

[4] Orsi RJ, Moore JB, Mahony RE. Spectrum estimation of interleaved pulse trains. IEEE T Signal Proces 1999; 47: 1646-1653.

[5] Conroy TL, Moore JB. On the estimation of interleaved pulse train phases. IEEE T Signal Proces 2000; 48: 3420-3425.

[6] Davies CL, Hollands P. Automatic processing for ESM. P IEEE Part F 1982; 129: 164-171.

[7] Mardia HK. New techniques for the deinterleaving of repetitive sequences. P IEEE Part F 1989; 136: 149-154.

[8] Milojevic DJ, Popovic BM. Improved algorithm for deinterleaving of radar pulses. P IEEE Part F 1992; 139: 98-104.

[9] Ray PS. A novel pulse TOA analysis technique for radar identification. IEEE T Aero Elec Sys 1998; 34: 716-721.

[10] Nishiguchi K, Kobayashi M. Improved algorithm for estimating pulse repetition intervals. IEEE T Aero Elec Sys 2000; 36: 407-421.

[11] Noone GP. A neural approach to automatic pulse repetition interval modulation recognition. In: Information, Decision and Control Conference; 8–10 February 1999; Adelaide, South Australia. New York, NY, USA: IEEE. pp. 213-218.

[12] Rong H, Jin W, Zhang C. Application of support vector machines to pulse repetition interval modulation recognition. In: 2006 6th International Conference on ITS Telecommunications; June 2006; Chengdu, China. New York, NY, USA: IEEE. pp. 1187-1190.

[13] Ryoo YJ, Song KH, Kim WW. Recognition of PRI modulation types of radar signals using the autocorrelation. IEICE T Commun 2007; 90: 1290-1294.

[14] Kauppi JP, Martikainen K, Ruotsalainen U. Hierarchical classification of dynamically varying radar pulse repetition interval modulation patterns. Neural Networks 2010; 23: 1226-1237.

[15] Hu G, Liu Y. An efficient method of pulse repetition interval modulation recognition. In: 2010 International Conference on Communications and Mobile Computing; 12–14 April 2010; Shenzhen, China. New York, NY, USA: IEEE. pp. 287-291.

[16] Mahdavi A, Pezeshk AM. A robust method for PRI modulation recognition. In: 2010 IEEE 10th International Conference on Signal Processing; 24–28 October 2010; Beijing, China. New York, NY, USA: IEEE. pp. 1873-1876.

[17] Song KH, Lee DW, Han JW, Park BK. Pulse repetition interval modulation recognition using symbolization. In: 2010 International Conference on Digital Image Computing: Techniques and Applications; 1–3 December 2010; Sydney, Australia. New York, NY, USA: IEEE. pp. 540-545.

[18] Keshavarzi M, Pezeshk AM, Farzaneh F. A new method for detection of complex pulse repetition interval modulations. In: 2012 IEEE 11th International Conference on Signal Processing; 21–25 October 2012; Beijing, China. New York, NY, USA: IEEE. pp. 1705-1709.

[19] Mallat S. A theory for multiresolution signal decomposition: the wavelet representation. IEEE Tran Pattern Anal 1989; 11: 674-693.

[20] Vetterli M, Kovacevic J. Wavelets and Subband Coding. Englewood Clifis, NJ, USA: Prentice Hall, 2007.

[21] Vapnik VN. An overview of statistical learning theory. IEEE T Neural Networ 1999; 10: 988-1000.

[22] Cortes C, Vapnik V. Support-vector networks. Mach Learn 1995; 20: 273-297.

[23] Müller KR, Mika S, Rätsch G, Tsuda K, Schölkopf B. An introduction to kernel-based learning algorithms. IEEE T Neural Networ 2001; 12: 181-201.

[24] Daubechies I. Ten Lectures on Wavelets. Philadelphia, PA, USA: SIAM, 1992.